Journal of Non-Crystalline Solids 407 (2015) 14–22

Contents lists available at ScienceDirect

Journal of Non-Crystalline Solids

journal homepage: www.elsevier.com/ locate/ jnoncrysol

A review of experiments testing the shoving model

Tina Hecksher *, Jeppe C. Dyre

DNRF Centre Glass and Time, IMFUFA, Department of Sciences, Roskilde University, Postbox 260, DK-4000 Roskilde, Denmark

ARTICLE INFO

Article history:
Received 1 June 2014
Received in revised form 20 August 2014
Available online 26 September 2014

Keywords:
Instantaneous shear modulus;
Glass-forming liquids;
Non-Arrhenius;
Relaxation time;
Viscosity

ABSTRACT

According to the shoving model the non-Arrhenius temperature dependence of supercooled liquids' relaxation time (or viscosity) derives from the fact that the high-frequency shear modulus is temperature dependent in the supercooled phase, often increasing a factor of three or four in the temperature interval over which the relaxation time increases by ten to fifteen decades. In this paper we have compiled all tests of the shoving model known to us. These involve rheological data obtained by different techniques, high-frequency sound-wave data, neutron scattering data for the vibrational mean-square displacement, data obtained at or below the glass transition, as well as data testing the model under out-of-equilibrium conditions, i.e., during aging. Most data confirm the model, some do not. We conclude that more work is needed to precisely characterize the model's range of applicability.

1. Introduction

All liquids can be supercooled without crystallizing when cooled fast enough. Upon continued cooling, the viscosity of the liquid increases enormously until the liquid eventually falls out of equilibrium and forms a glass. This dramatic increase of viscosity found in supercooled liquids is the true mystery of glass science, not what happens at the actual glass transition or why it takes place. After all, any system with an extremely long relaxation time is bound to fall out of equilibrium upon cooling whenever this process increases the relaxation time beyond any limits.

A number of empirical models, as well as first principle theories, have been developed over the years to account for the super-Arrhenius behavior of glass-forming liquids. Most of these models take their starting point in a thermally activated picture, i.e., in the Arrhenius model predicting $\gamma(T) = \gamma_0 exp(-\Delta E/k_B T)$ in which the temperature dependence of some rate γ – for instance a reaction rate – is given as an attempt frequency γ_0 times a Boltzmann factor. In this framework, the question of the origin of the super-Arrhenius behavior of glass-forming liquids' relaxation time becomes a question of the origin of the temperature dependence of the free energy barrier. In particular: Why is the barrier seldom temperature independent, but is virtually always increasing upon cooling?

In this paper we review experimental tests of one model for the non-Arrhenius behavior of glass-forming liquids, the phenomenological so-called shoving model [1,2]. This is one example out of several closely related "elastic" models for supercooled liquid dynamics. As reviewed in Ref. [2], elastic models connect the short and long time scales via the following philosophy: Relaxation is slow because the barriers to be overcome for a molecular rearrangement are large. The barrier transition itself, however, is a fast process. What happens here may well be determined by the system's short-time properties, for instance its elastic constants probed on the short time scale.

The paper is structured as follows. After recapitulating the basic assumptions of the shoving model, we proceed to describe the different ways in which the model has been tested. The tests are divided into "themes": dynamic rheology measurements of the frequency-dependent shear modulus and viscosity, sound-velocity measurement at high frequencies (>100 kHz), measurements of the mean-square displacement, tests performed at and below the glass transition temperature, and finally a few studies where the model was tested in out-of-equilibrium situations. We end by compiling all tests of the shoving model (known to us) into a table.

2. The shoving model

Like most phenomenological models of viscous flow, the shoving model is based on the idea that viscous flow proceeds via a series of "flow-events" that are themselves fast, but as the liquid is cooled become progressively rarer. In the deeply supercooled state, the molecules of the liquid spend most of the time vibrating around a fixed position just like in a solid, interrupted by occasional jumps to a new position. This picture was proposed by Goldstein [3] and has later been confirmed by computer simulations (see, e.g., Ref. [4]).

In the shoving model, it is argued that it is energetically costly for the molecules to rearrange at constant volume because of the anharmonicity of the intermolecular potential. This is steeply repulsive, meaning that it is energetically very costly to "squeeze" molecules past each other if the surrounding molecules stay in place and do not move. A flow event is

* Corresponding author.
E-mail address: tihe@ruc.dk (T. Hecksher).

http://dx.doi.org/10.1016/j.jnoncrysol.2014.08.056
0022-3093/

much more likely to happen when a thermal fluctuation creates a local volume increase, because this lowers the energy barrier for a molecular rearrangement. A further effect of the intermolecular potential's anharmonicity is that the main contribution to the barrier comes from the work done in shoving aside the surrounding molecules to create a local volume increase (recall from statistical mechanics that the probability of this happening by a thermal fluctuation is governed by the free-energy increase calculated as the reversible work done to make the same change).

Since a flow event is fast, the surrounding liquid behaves like a solid during this expansion. The simplest model of this is a spherically symmetric elastic expansion taking place in an isotropic continuous elastic medium. Such a medium is characterized by just two fundamental elastic constants, the shear modulus G and the bulk modulus K (the latter exists in both an isothermal and an adiabatic version). A standard exercise in elasticity theory shows that a sphere expanded radially in such a medium does not compress any parts of its surroundings. What happens is that the radial displacement field varies with the distance from the sphere center r as $\propto 1/r^2$. This is a pure shear displacement field, i.e., a vector field with zero divergence, compare Gauss' law for the Coulomb electric field. Thus the only relevant elastic constant is G. But since it should correspond to the liquid's elasticity probed on a short time scale, the notation G_∞ is traditionally used — in fact any liquid by definition has zero low-frequency limit of the shear modulus.

In summary, the shoving model predicts that the energy barrier to be overcome for a molecular rearrangement is dominated by the elastic work done in "shoving aside" the surrounding molecules. This work is proportional to the short-time elastic constant G_∞. Thus the model predicts that the temperature dependence of the relaxation time (or viscosity) is given by

$$\tau(T) = \tau_0 exp\left\{\frac{V_c G_\infty(T)}{k_B T}\right\}. \tag{1}$$

There is no a priori reason to assume that the characteristic volume V_c, which is a microscopic volume of molecular size, is constant when temperature changes. Many years after the shoving model was proposed, however, the isomorph theory predicted that if an equation like Eq. (1) applies, V_c must scale as one over density, i.e., be virtually constant [5]. Assuming that V_c is temperature independent, the logarithm of the relaxation time is predicted to be a linear function of $G_\infty(T)/T$,

$$ln\left(\frac{\tau(T)}{\tau_0}\right) = \frac{V_c G_\infty(T)}{k_B T}. \tag{2}$$

At the glass transition it follows that

$$ln\left(\frac{\tau\left(T_g\right)}{\tau_0}\right) = \frac{V_c G_\infty\left(T_g\right)}{k_B T_g}. \tag{3}$$

Before proceeding we note that G_∞ is the physically measurable shear modulus corresponding to measurements on a time scale short enough that the frequency-dependent complex shear modulus $G(\omega)$ is virtually constant, a constant that is often referred to as the plateau modulus. This is a frequency-independent, real number. There was recently some controversy about this issue [6,24]. The confusion derived from the fact that, whereas traditionally in experiment G_∞ has always been understood as the quantity discussed above, in liquid-state theory G_∞ is traditionally a different quantity. The issue was discussed and clarified in Ref. [24]. Thus, in Ref. [6], G_∞ is the modulus referring to the thought experiment of a perfectly affine deformation of the system carried out infinitely fast, i.e., on a time scale much faster than the phonon time scale. This cannot be done in an experiment, but is easily done, e.g., in a computer simulation. Likewise, this quantity is readily evaluated theoretically, for instance from the radial distribution function. This quantity typically decreases upon cooling, whereas the experimental plateau modulus G_∞ typically increases.

If we divide Eq. (2) by Eq. (3), assuming that V_c is temperature independent, we obtain after rearranging

$$ln\,\tau(T) = \left[ln\frac{\tau\left(T_g\right)}{\tau_0}\right]\frac{G_\infty(T)}{T}\frac{T_g}{G_\infty\left(T_g\right)} + ln\,\tau_0. \tag{4}$$

Defining the parameter [1]

$$X \equiv \frac{G_\infty(T)T_g}{G_\infty\left(T_g\right)T} \tag{5}$$

and the glass transition temperature T_g in the standard way by $\tau(T_g) = 100$ s, if the prefactor is given by $\tau_0 = 10^{-14}$ s, we arrive at the following shoving-model prediction

$$log\,\tau(T) = 16X - 14. \tag{6}$$

Here X runs from zero for $T \to \infty$ to unity at $T = T_g$. This gives rise to "shoving plots" for testing the model without any free parameters.

3. Five different ways of testing the shoving model

In this section we review different model tests found in the literature. Each subsection deals with either a specific measurement type or a specific conceptual idea for applying/testing the model.

3.1. Rheology

In rheological measurements the frequency-dependent shear viscosity (or, equivalently, the shear modulus) is measured directly. Thus in principle $G_\infty(T)$ can be determined as the high-frequency plateau of the shear-modulus $G(\omega)$. However, rheological techniques generally have a limited (and rather low) frequency window available. For this reason, for a highly viscous liquid the high-frequency plateau is only within the measuring window when the liquid is close to its glass transition temperature.

The real and imaginary parts of the shear modulus are connected through the Kramers–Kronig relation

$$G'(\omega) = \frac{2}{\pi}\int_0^\infty \frac{\omega' G''(\omega')}{\omega'^2 - \omega^2} d\omega' \tag{7}$$

which implies that

$$G_\infty = \lim_{\omega\to\infty} G'(\omega) = 2/\pi\int_{-\infty}^{\infty} G''(\omega) d\,ln\,\omega. \tag{8}$$

G_∞ is proportional to the maximum loss if the liquid obeys time–temperature superposition (TTS) for the dynamic shear modulus $G(\omega)$, $G_\infty(T) \propto G''_{max}(T)$. In this case it is possible to evaluate the variable X directly from the data without analytical extrapolations of any kind.

This method of testing the model has been used mainly by our group, compare Refs. [1,8,9] that give data for a range of organic molecular liquids, the type of liquid best suited for our experimental setup using a piezoceramic shear transducer [10]. All liquids tested so far follow Eq. (5) to a reasonably good approximation when the logarithm of the relaxation time is plotted against the parameter X, see Fig. 1(a) for an early example.

The proportionality of $G''_{max}(T)$ with $G_\infty(T)$ when there is TTS also makes it possible to test the model by plotting the loss spectra divided by temperature, see Fig. 1(b). In this representation the axes of the "shoving plot" of Fig. 1(a) are swopped, and the peak positions on the x-axis give a characteristic time for the structural relaxation while

the y-axis identifies $G''_{max}(T)/T$ as the peak (proportional to $G_\infty(T)/T$). The advantage of this plot is that it shows all actual data points, emphasizing the fact that both the characteristic relaxation time and the instantaneous shear modulus G_∞ (or its equivalent $G''_{max}(T)$) are determined from one and the same data set. This approach was used in Refs. [11,12].

Xu and McKenna [13] compared the shoving model's ability to predict the relaxation time at temperatures below T_g, i.e., for relaxations in the glassy phase, to that of the VFT model. This was done by extrapolating $G_\infty(T)$ measured by rheology above T_g and fitting V_c and τ_0 to these data, compare Fig. 1(c). Their conclusion was that the shoving model gives a more reasonable extrapolation below T_g than the VFT mathematical equation.

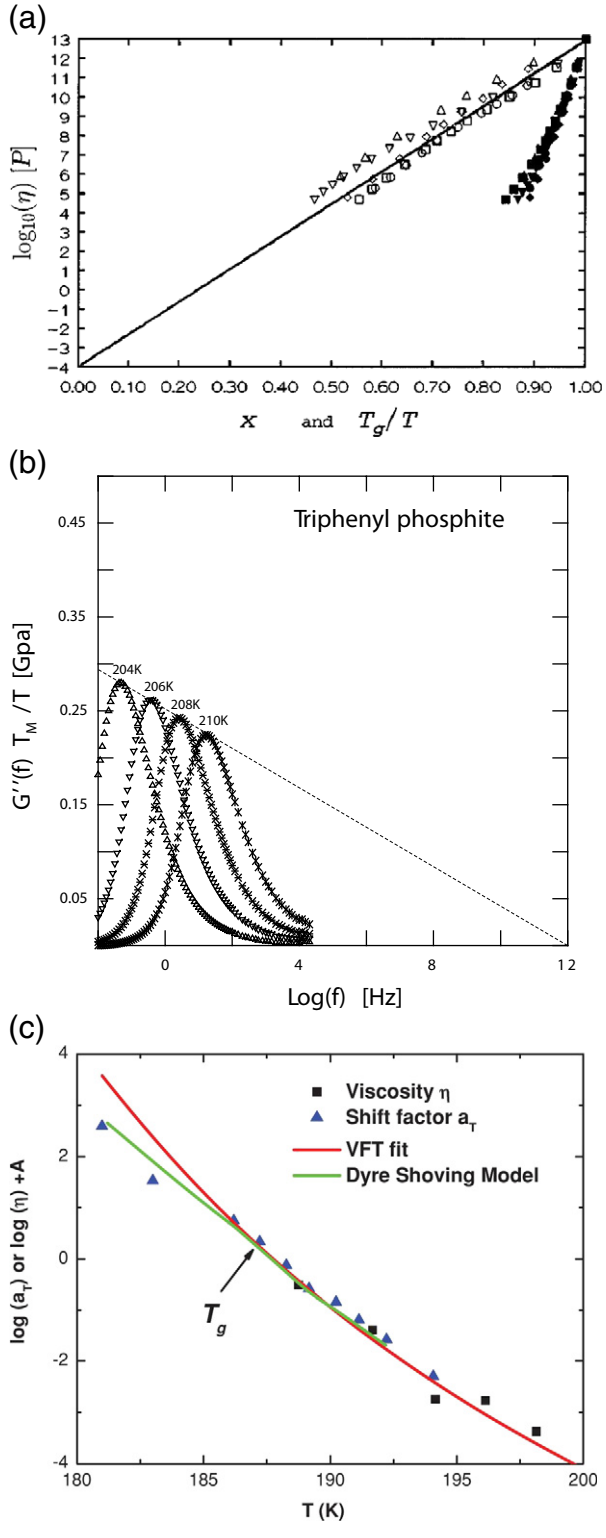

Fig. 1. Different tests of the shoving model by rheological methods, in which (a) and (b) assume time–temperature superposition. (a) Full symbols show the viscosity plotted as a function of the inverse temperature scaled by T_g (the standard Angell fragility plot), open symbols show the same quantity plotted against the parameter X of Eq. (5). The model predicts a straight line connecting the value at the glass transition (defined by $\eta = 10^{13}$ P) with the high-temperature prefactor (the number 16 in Eq. (6) is here 17) (reproduced from Ref. [1]). (b) The imaginary part of shear-modulus spectra at different temperatures scaled by temperature (normalized to a high temperature), $G''(\omega)T_M/T$. In terms of this quantity the model predicts that the maxima extrapolate linearly to zero at the attempt frequency, which cannot be far from 0.1 ps in order to be physically reasonable (reproduced from Ref. [11]). (c) Extrapolation via the shoving model to estimate the relaxation rate below the glass transition (green curve), compared to the prediction of the mathematical VFT equation (red curve). The black dots are data points (reproduced from Ref. [13]).

3.2. Sound waves

Classical ultrasonic measurements and light scattering experiments probe directly the propagation of sound waves in the liquid. The sound velocity is closely related to the mechanical moduli as we briefly review below.

The general equation of motion for an isotropic medium is given [14] by

$$\rho\ddot{\mathbf{u}} = (K + 4/3G)\nabla(\nabla\cdot\mathbf{u}) - G\nabla\times\nabla\times\mathbf{u}. \tag{9}$$

Here $\mathbf{u}$ is the displacement field, ρ is the density, K and G are the bulk and shear moduli, and dot means differentiation with respect to time. Assuming a one-dimensional (longitudinal) geometry we have $\mathbf{u} = (u_x(x,t), 0, 0)$ and Eq. (9) reduces to

$$\rho\ddot{u}_x = Mu''_x. \tag{10}$$

The prime here means differentiation with respect to x and $M \equiv K + 4/3G$ is the so-called longitudinal modulus.

Assuming a harmonic input the displacement field can be written as

$$u(x,t) = u_0 e^{i(kx-\omega t)} = u_0 e^{ik(x-(\omega/k)t)} \tag{11}$$

where the (longitudinal) phase velocity of the wave is given by $c_l = \omega/k$. Inserting this into Eq. (10) we get

$$\rho\omega^2 = Mk^2 \quad\Rightarrow\quad c_l = \sqrt{M/\rho}. \tag{12}$$

If there is dispersion in the medium M is complex and frequency dependent and the wavevector k is complex. Writing $k = k' + ik''$ we have

$$e^{i(kx-\omega t)} = e^{i((k'+ik'')x-\omega t)} = e^{i(k'x-\omega t)}e^{-k''x}. \tag{13}$$

Eq. (12) still applies when k is complex, leading to

$$\omega/k = \sqrt{M(\omega)/\rho}. \tag{14}$$

From this one defines the (longitudinal) sound velocity as $c_l \equiv \omega/k'$, i.e., as the phase velocity of the wave, and one defines the damping coefficient as k''. Using Eq. (12) we get expressions for the frequency-dependent sound velocity c_l and the acoustic damping, traditionally denoted by α,

$$\begin{aligned} c_l(\omega) &= \frac{\omega}{k'(\omega)} = \frac{1}{\mathrm{Re}\left\{\sqrt{\frac{\rho}{M(\omega)}}\right\}}, \\ \alpha(\omega) &= k''(\omega) = \omega\,\mathrm{Im}\left\{\sqrt{\frac{\rho}{M(\omega)}}\right\}. \end{aligned} \tag{15}$$

Conversely, if one wishes to calculate the modulus from a complex wave vector k at a given frequency ω, then by Eq. (14) we have

$M(\omega) = \rho\omega^2/k^2$ implying

$$M(\omega) = \frac{\rho\omega^2\left(k'^2 - k''^2\right)}{|k|^4} - i\frac{2\rho\omega^2 k' k''}{|k|^4}. \quad (16)$$

In the high-frequency limit, if the damping vanishes, i.e., $\alpha = k''(\omega \to \infty) \to 0$), this reduces to

$$M_\infty = \rho c_{l,\infty}^2 . \quad (17)$$

Analogously, for the high-frequency shear modulus and the high-frequency transverse sound velocity c_s one obtains

$$G_\infty = \rho c_{s,\infty}^2 . \quad (18)$$

In both expressions the density ρ and the limiting sound velocities are both in general functions of the temperature.

Measurements of the sound velocity at a fixed frequency as a function of temperature in the equilibrium liquid show an s-shaped transition. The position of the transition depends on the frequency monitored: at high frequencies the transition happens at a higher temperature than at lower frequencies. In Fig. 2 an example of such data (for glycerol) is shown.

Incidentally, from this figure an often overlooked fact is evident: when a liquid forms a glass, the temperature dependence of the sound velocity becomes much less pronounced. This means that one cannot make the identification $c_{\text{glass}}(T) \cong c_\infty(T)$, as is sometimes done — if this identification is made, the term "glass" refers to a state that changes with temperature. One can only meaningfully make the identification $c_{\text{glass}} \cong c_\infty(T = T_g)$ which assumes (correctly) that the sound velocity is not very temperature dependent in the glass phase.

Venkateshan & Johari [16] monitored the evolution of the transverse sound velocity during polymerization of a mixture of diglycidyl ether of bisphenol-A (DGEBA) and diethylenetriamine (DETA) by means of Brillouin scattering. They found a linear relation between $log\tau$ and the square of the transverse sound velocity. This is predicted by the shoving model (provided that the density of the mixture does not change significantly during the polymerization process), compare Eq. (18).

High-frequency sound velocity measurements date back in time to (at least) the 1950s. The nice book by Harrison [17] summarizes much of this work, and it should be noted that some of these old data were used in the original shoving model paper from 1996 [1].

In Ref. [18] Torchinsky et al. measured the transverse sound velocity by the transient grating method (i.e., by impulsive stimulated Brillouin scattering) and combined these data with literature values for the relaxation time. The method gives the sound velocity in the high MHz region. By assuming that this frequency is high enough to probe the non-dispersive high-frequency properties of the liquid at all temperatures, these authors obtained shoving plots of the data in good agreement with the model.

A recently developed technique is Picosecond Ultrasonic Interferometry, which enables excitation and subsequent detection of the propagation of transverse sound waves in the 10–50 GHz range. Klieber et al. [19] measured the temperature dependence of transverse sound velocity of DC704 and glycerol by this method and found that the data largely confirm the shoving model.

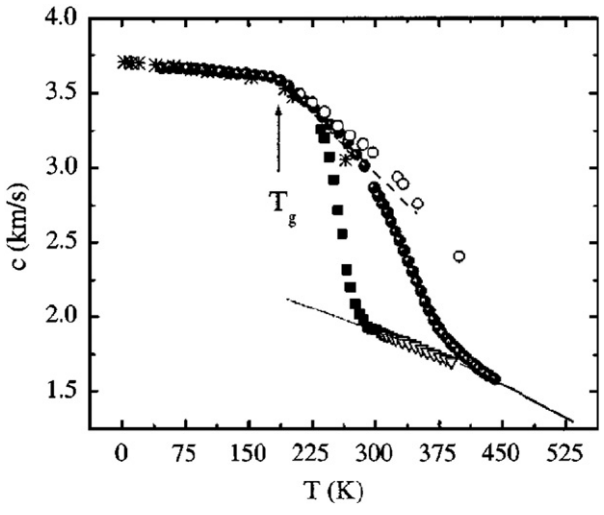

Fig. 2. Longitudinal sound velocity of glycerol as a function of temperature for different frequecies/wavevectors (reproduced from Ref. [15]).

3.3. Mean-square displacement

In Ref. [20] an energy-landscape equivalent of the shoving model was proposed. The idea is that the curvature at the bottom of the energy landscape by quadratic extrapolation determines the barrier height. If $\langle u^2\rangle$ is the vibrational mean-square displacement, this leads to the prediction for the relaxation time $\tau \propto exp(C/\langle u^2\rangle)$, or in terms of the activation energy $\Delta E(T) \propto k_B T/\langle u^2\rangle$. In terms of the mechanical moduli, because there are two transverse and one longitudinal phonon for each wavevector, one has [20]

$$\left\langle u^2\right\rangle \propto T(2/G + 1/M). \quad (19)$$

Combining this with $\Delta E(T) \propto k_B T/< u^2 >$ leads to

$$\frac{1}{\Delta E(T)} \propto \frac{2}{G_\infty(T)} + \frac{1}{M_\infty(T)}. \quad (20)$$

In this expression the temperature dependence of the shear modulus dominates over that of the bulk modulus because (1) the shear modulus is weighted doubly, (2) the shear modulus also enters into the longitudinal modulus $M = K + 4/3G$, and (3) the longitudinal modulus is larger than the shear modulus ($M > G$) for which reason longitudinal phonons contribute less than 1/3 to the temperature variation of $\Delta E(T)$. In fact, within these model assumptions it can be shown rigorously that the bulk modulus accounts for at most 8% of the temperature dependence of $\Delta E(T)$ [20].

The temperature index of the activation energy [21] is defined as

$$I_{\Delta E} = -\frac{d\ ln\ \Delta E}{dlnT} \quad (21)$$

which is related to the fragility $m = \left.\frac{d\ log\tau}{d(T_g/T)}\right|_{T_g}$ through the following relation [21] (where $\tau_g = \tau(T_g)$)

$$m = log\left(\frac{\tau_g}{\tau_0}\right)\left(1 + I_{\Delta E}\left(T_g\right)\right) = log\left(\frac{\tau_g}{\tau_0}\right)\left.\frac{d\ ln\left\langle u^2\right\rangle}{d\ lnT}\right|_{T_g}. \quad (22)$$

Thus according to the shoving model the fragility m and the logarithmic derivative of $\langle u^2\rangle$ are proportional and the constant of proportionality is $log(\tau_g/\tau_0) \cong 16$ (see Eq. (6)).

This approach was employed by Niss et al. [22], who compared literature values of the fragility index m with neutron-scattering measurements of the temperature dependence of $\langle u^2\rangle$. They found for a number of liquids that this prediction is followed to a good approximation when $\langle u^2\rangle$ was measured on the nanosecond time-scale, but that significant deviations occur when $\langle u^2\rangle$ was measured on a faster time scale.

A famous study by Larini et al. from 2008 [23] compiled literature data for the mean-square displacement and relaxation times for number of viscous liquids and polymers. The focus of this paper was not on testing the shoving model. The main figure in the paper shows the relaxation time on a logarithmic scale as a function of the

inverse of the mean-square displacement (reproduced in Fig. 3). In this plot, the energy-landscape equivalent of the shoving model predicts that $log\tau$ depends linearly on $1/\langle u^2\rangle$, which is clearly not the case.

3.4. Measurements at and below T_g

Measuring the frequency-dependent mechanical moduli of a liquid is notoriously difficult, whereas measuring the static moduli of a solid is relatively easy. The philosophy of Dyre & Wang [24] was to make use of an already existing catalogue of data for the shear and bulk moduli of several metallic glasses. In order to arrive at a zero-adjustable-parameter test, they made the following simplifying assumptions: (1) at a fixed cooling rate $\tau(T_g)$ is fixed across different samples, (2) the glass shear modulus does not change much with temperature, meaning that one can use $G(T<T_g)\cong G_\infty(T_g)$ for estimating the latter quantity, and (3) the characteristic volume V_c in the shoving model is proportional to the molar volume $V_c\propto V_m$ with the same constant of proportionality for all the systems studied. From these assumptions, the shoving model prediction is that for glasses prepared by similar cooling rates [24]

$$\frac{GV_m}{RT_g}\simeq \text{Const.} \tag{23}$$

The results for several bulk metallic glasses are reproduced in Fig. 4. Eq. (23) is almost fulfilled (upper subfigure), but there is a slight correlation with the Poisson's ratio. Replacing the shear modulus in Eq. (23) by the bulk modulus, the correlation is much stronger. Interestingly, the energy landscape "equivalent" of the shoving modulus (Eq. (20)) gives a constant value independent of Poisson's ratio (lower subfigure).

Compiling Brillouin scattering literature data for a number of liquids Buchenau [25] evaluated the temperature index of the activation energy defined by Eq. (21) and this quantity's relation to the fragility index (Eq. (22)) as well as the temperature index of the shear modulus

$$I_{G_\infty}=-\left.\frac{d\ lnG_\infty}{d\ lnT}\right|_{T=T_g}. \tag{24}$$

The shoving model predicts that $I_{\Delta E}=I_{G_\infty}$ if V_c as usual is assumed constant. In general, Buchenau found $I_{G_\infty}<I_{\Delta E}$, leading to the conclusion that the temperature dependence of the shear modulus is not enough to explain the non-Arrhenius temperature dependence of relaxation time, i.e., the data do not conform to the shoving model prediction.

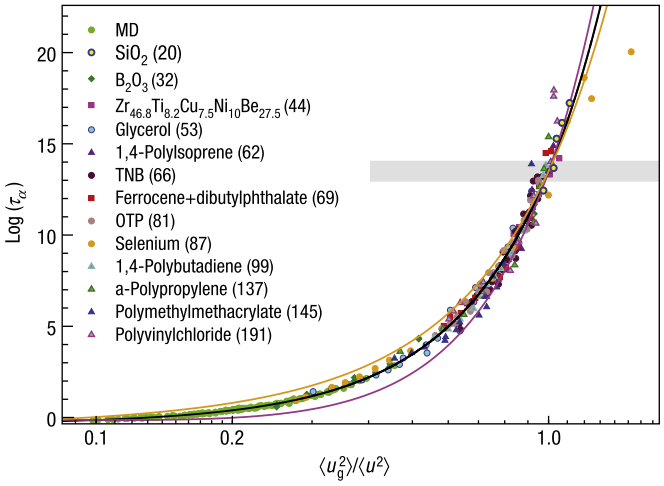

Fig. 3. Compilation of literature data for the relaxation time and the vibrational mean-square displacement. The shoving model predicts a linear relationship which is not obeyed for these data (reproduced from Ref. [23]).

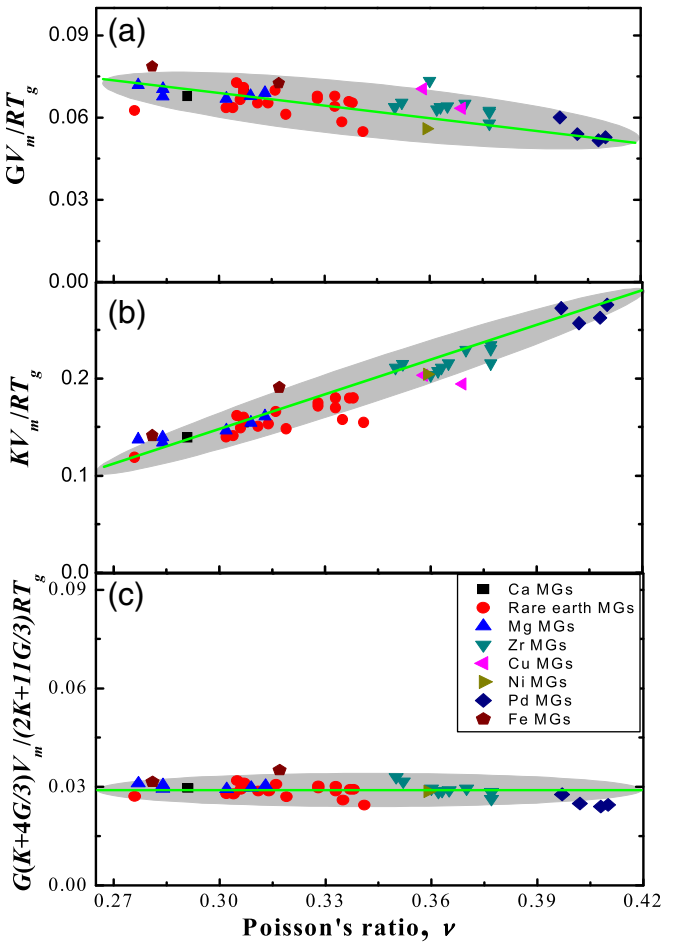

Fig. 4. Comparing shoving model predictions to data for several metallic glasses. (a) Test of Eq. (23), where G is the glass shear modulus which is reasonably well obeyed though there is a weak correlation to the Poisson ratio. (b) This correlation is of opposite sign and much more pronounced if the bulk modulus is used as the elastic constant of the model. (c) The energy-landscape analogue of the shoving model, corresponding to replacing G in Eq. (23) by an effective G defined from Eq. (20), gives the best fit to data. (reproduced from Ref. [24]).

3.5. Out-of-equilibrium

The shoving model has been applied to liquids not in thermal equilibrium in two different ways.

Olsen et al. [26] performed an isothermal aging experiment monitoring the instantaneous shear modulus as a function of time after a temperature step, $G_\infty(t)$. By assuming that the shoving model's expression for the relaxation time applies also for this aging experiment, an expression for the time-dependent relaxation time is obtained. Applying the Tool–Narayanaswamy [27,28] formalism is now straightforward, since the reduced time

$$\tilde{t}=\int_\infty^t \frac{dt'}{\tau(G_\infty(t'))} \tag{25}$$

is readily obtained from the experimental data. The relaxation curves from two different temperature jumps to the same temperature, one up-jump and one down-jump, collapse when plotted as functions of the reduced time. Thus the extension of the shoving to model was validated.

Potuzak et al. [29] applied a similar approach by formulating the time-dependence in terms of a fictive temperature, using

$$\tau\left(T,T_f\right)=\tau_0\,exp\left(\frac{V_cG_\infty\left(T,T_f\right)}{kT}\right) \tag{26}$$

Table 1
List of liquids tested. The first column gives the name of the liquid, the second column gives the reference to the work in which the comparison was made, third column gives the reference to where the used data are published, fourth column is the method used for obtaining the mechanical data (rheology: RHE, Brillouin scattering: BRI, Mssbauer spectroscopy: MS, incoherent neutron scattering: INS, ultrasonics: US, picosecond ultrasonic interferometry: PUI, some type of resonant method (or direct mechanical vibration method): RES), and the fifth column indicates whether the test was found to be in support of the shoving model (⊙), in conflict with the shoving model (⊗) or inconclusive (⊖). Some liquids were tested more than once (by different measurements and/or methods) usually with the same conclusion (i.e., DC704), but sometimes also with disparate conclusions (i.e., in the case of glycerol). There is a rather long list of bulk metallic glasses due the simple way of testing the model used in this case (based on measuring the glass' transition temperature, its static shear modulus, and its molar volume, compare Eq. (23)). The data references are reproduced from the cited original work in column two, but some citations were in error and have been corrected. Wherever the reference cited could not be located, the reference in column two is repeated. Most bulk metallic glass data from Ref. [24] can be found in Ref. [7]. For some of these, the original references are older; they are marked with an *. For a few of the bulk metallic glasses we were not able to locate the data reference. In that case we have referred Ref. [109], which contains a table with more details than Ref. [24].

Liquid	Ref.	Data	Meth.	Supp.
4-Methylpentane-2-ol	[1]	[1]	RHE	⊙
Dioctyl phthalate	[1]	[1]	RHE	⊙
Salol	[1]	[1]	RHE	⊙
Dibutyl phthalate	[1]	[1]	RHE	⊙
DC704	[1]	[1]	RHE	⊙
Isopropyl-benzene	[1]	[35]	US	⊙
n-Propyl-benzene	[1]	[35]	US	⊙
Sec-butyl-benzene	[1]	[35]	US	⊙
Di-(isobutyl)-phthalate	[1]	[35]	US	⊙
Di-(*n*-butyl)-phthalate	[1]	[35]	US	⊙
Di-(2 ethyl hexyl)-phthalate	[1]	[35]	US	⊙
5-phenyl-4-ether	[1]	[36]	BRI	⊙
α-Phenyl-o-cresol	[1]	[37,38]	BRI	⊙
DC704	[26]	[26]	RES	⊙
$Pd_{40}Ni_{40}P_{20}$	[39]	[39]	RES	⊙
Triphenyl-ethylene	[8]	[8]	RHE	⊙
5-Phenyl-4-ether	[8]	[8]	RHE	⊙
DGEBA-DETA mixture	[16]	[16]	BRI	⊙
Triphenyl-phosphite	[11]	[11]	RHE	⊙
5-Phenyl-4-ether	[11]	[11]	RHE	⊙
$Zr_{46.25}Ti_{8.25}Cu_{7.5}Ni_{10}Be_{27.5}$	[40]	[40]	US	⊗
1,2-Propanediol	[9]	[9]	RHE	⊙
DC705	[9]	[9]	RHE	⊙
SiO_2	[23]	[41,42]	INS	⊗
B_2O_3	[23]	[43–45]	INS	⊗
$Zr_{46.8}Ti_{8.2}Cu_{7.5}Ni_{10}Be_{27.5}$	[23]	[46,47]	MS	⊗
Glycerol	[23]	[48,49]	INS	⊗
1,4-Poly isoprene	[23]	[50,51]	INS	⊗
TNB	[23]	[52,53]	INS	⊗
Ferrocene/DBP	[23]	[54,55]	MS	⊗
OTP	[23]	[53,56]	INS	⊗
Selenium	[23]	[57]	INS	⊗
1,4-Polybutadiene	[23]	[58–60]	INS	⊗
a-Polypropylene	[23]	[61,62]	INS	⊗
Polymethylmethacrylate	[23]	[63,64]	INS	⊗
Polyvinylchoride	[23]	[65,64]	INS	⊗
2-Benzylphenol/OTP	[18]	[66,38,18]	ISS	⊙
5-Phenyl-4-ether	[18]	[36,18]	ISS	⊙
DC704	[18]	[18]	ISS	⊙
m-Flouroaniline	[18]	[67,18]	ISS	⊙
Salol	[18]	[68,66,18]	ISS	⊙
m-toluidine	[18]	[69,70,18]	ISS	⊙
Diethyl-phthalate	[18]	[71,18]	ISS	⊙
Triphenyl-phosphite	[18]	[72,18]	ISS	⊙
$Ca(NO)_3 \cdot H_2O$	[18]	[73,18]	ISS	⊙
$Pd_{40}Cu_{30}Ni_{30}P_{30}$	[74]	[74]	RES	⊙
Silica	[25]	[75,76]	BRI	⊗
$Zr_{46.25}Ti_{8.25}Cu_{7.5}Ni_{10}Be_{27.5}$	[25]	[40]	US	⊗
Glycerol	[25]	[77–79]	BRI/US	⊗
Polybutadiene mixture	[25]	[78,80–82]	RHE	⊗
$K_3Ca_2(NO_3)_7$ (CKN)	[25]	[78,83]	BRI	⊗
Bisphenol-A-polycarbonate	[25]	[78,84,81,85]	BRI	⊗
Polystyrene	[25]	[78,86,87,81,88]	RHE	⊗
PMMA	[25]	[78,89,81,90]	BRI	⊗
Decahydro-isoquinoline	[22]	[91,92,22]	INS	⊖
Glycerol	[22]	[22]	INS	⊖
Dibuthylphtalate	[22]	[22]	INS	⊖
Orthoterphenyl	[22]	[22]	INS	⊙
m-Toluidine	[22]	[22]	INS	⊙
Cumene	[22]	[93,22]	INS	⊙
Triphenyl-phosphite	[22]	[94,22]	INS	⊙
Sorbitol	[22]	[95,22]	INS	⊙
m-toluidine	[13]	[96]	RHE	⊙
Sucrose-benzoate	[13]	[96]	RHE	⊙
a-Se	[31]	[97]	RES	⊙
$GeSe_4$	[31]	[98,97]	RES	⊙
$GeSe_3$	[31]	[98,97]	RES	⊙
Ge_3Se_7	[31]	[98,97]	RES	⊙
Glycerol	[31]	[77,99]	US	⊙
a-SiO_2	[31]	[100,97]	US	⊙
ZBLAN	[31]	[101]	US	⊙
B_2O_3	[31]	[102]	BRI	⊙
$Ca_3Al_2Si_3O_{12}$	[31]	[103]	BRI	⊙
$CaAl_2Si_2O_8$	[31]	[103]	BRI	⊙
$Zr_{55}Cu_{30}Al_{10}Ni_5$	[31]	[104]	US	⊙
Aluminosilicate 1	[31]	[31]	US	⊙
Aluminosilicate 2	[31]	[31]	US	⊙
$CaMgSi_2O_6$	[31]	[103]	BRI	⊙
$Pd_{42.5}Ni_{71}Cu_{30}P_{20}$	[31]	[105]	RES	⊙
Window glass	[31]	[106]	US	⊙
Oxynitride glass 1	[31]	[107,108]	US	⊙
Oxynitride glass 2	[31]	[107,108]	US	⊙
Propylene carbonate	[12]	[12]	RHE	⊙
NEA/NMF	[12]	[12]	RHE	⊙
$Ca_{65}\ Mg_{8.54}\ Li_{9.96}\ Zn_{16.5}$	[24]	[7]	US	⊙
$Ca_{65}\ Mg_{8.31}\ Li_{9.69}\ Zn_{17}$	[24]	[7]	US	⊙
$Yb_{62.5}\ Zn_{15}\ Mg_{17.5}\ Cu_5$	[24]	[7]*	US	⊙
$Ce_{70}\ Al_{10}\ Ni_{10}\ Cu_{10}$	[24]	[7]*	US	⊙
$(Ce_{20}\ La_{80})_{68}\ Al_{10}\ Cu_{20}\ Co_2$	[24]	[7]*	US	⊙
$Ce_{68}\ Al_{10}\ Cu_{20}\ Nb_2$	[24]	[7]*	US	⊙
$(Ce_{80}\ La_{20})_{68}Al_{10}\ Cu_{20}\ Co_2$	[24]	[7]*	US	⊙
$Ce_{68}\ Al_{10}\ Cu_{20}\ Co_2$	[24]	[7]*	US	⊙
$Ce_{68}\ Al_{10}\ Cu_{20}\ Co_2$	[24]	[7]*	US	⊙
$La_{60}\ Al_{20}\ Co_{20}$	[24]	[7]*	US	⊙
$Pr_{55}\ Al_{25}\ Co_{20}$	[24]	[7]*	US	⊙
$Dy_{55}\ Al_{25}\ Co_{20}$	[24]	[7]*	US	⊙
$Tb_{55}\ Al_{25}\ Co_{20}$	[24]	[7]*	US	⊙
$Ho_{55}\ Al_{25}\ Co_{20}$	[24]	[7]*	US	⊙
$Er_{55}\ Al_{25}\ Co_{20}$	[24]	[7]*	US	⊙
$Tm_{39}\ Y_{16}\ Al_{25}\ Co_{20}$	[24]	[7]*	US	⊙
$Tm_{55}\ Al_{25}\ Co_{20}$	[24]	[7]*	US	⊙
$Lu_{39}\ Y_{16}\ Al_{25}\ Co_{20}$	[24]	[7]*	US	⊙
$Lu_{45}\ Y_{10}\ Al_{25}\ Co_{20}$	[24]	[7]*	US	⊙
$Lu_{55}\ Al_{25}\ Co_{20}$	[24]	[7]*	US	⊙
$Mg_{65}\ Cu_{25}\ Gd_{10}$	[24]	[7]*	US	⊙
$Mg_{65}\ Cu_{25}\ Y_9\ Gd_1$	[24]	[109]	US	⊙
$Mg_{65}\ Cu_{25}\ Y_{10}$	[24]	[109]	US	⊙
$Mg_{65}\ Cu_{25}\ Y_8\ Gd_2$	[24]	[109]	US	⊙
$Mg_{65}\ Cu_{25}\ Y_5\ Gd_5$	[24]	[109]	US	⊙
$Mg_{65}\ Cu_{25}\ Tb_{10}$	[24]	[7]*	US	⊙
$Zr_{64.13}\ Cu_{15.75}\ Ni_{10.12}\ Al_{10}$	[24]	[109]	US	⊙
$Zr_{65}\ Cu_{15}\ Ni_{10}\ Al_{10}$	[24]	[109]	US	⊙
$Zr_{61.88}\ Cu_{18}\ Ni_{10.12}\ Al_{10}$	[24]	[109]	US	⊙
$Zr_{55}\ Al_{19}\ Co_{19}\ Cu_7$	[24]	[109]	US	⊙
$Zr_{57}\ Nb_5\ Cu_{15.4}\ Ni_{12.6}\ Al_{10}$	[24]	[7]	US	⊙
$Zr_{57}\ Ti_5\ Cu_{20}\ Ni_8\ Al_{10}$	[24]	[110]	US	⊙
$(Zr_{59}\ Ti_6\ Cu_{22}\ Ni_{13})_{85.7}\ Al_{14.3}$	[24]	[109]	US	⊙
$Cu_{45}\ Zr_{45}\ Al_7\ Gd_3$	[24]	[7]*	US	⊙
$Zr_{46.75}\ Ti_{8.25}\ Cu_{10.15}\ Ni_{10}\ Be_{27.25}$	[24]	[111]	US	⊙
$Zr_{48}\ Nb_8\ Cu_{12}\ Fe_8\ Be_{24}$	[24]	[7]*	US	⊙
$Zr_{41}\ Ti_{14}\ Cu_{12.5}\ Ni_{10}\ Be_{22.5}$	[24]	[111]	US	⊙
$Ni_{45}\ Ti_{20}\ Zr_{25}\ Al_{10}$	[24]	[110]	US	⊙
$Cu_{60}\ Zr_{20}\ Hf_{10}\ Ti_{10}$	[24]	[7]*	US	⊙
$Pd_{77.5}\ Cu_6\ Si_{16.5}$	[24]	[111]	US	⊙
$Pd_{64}\ Ni_{16}\ P_{20}$	[24]	[7]*	US	⊙
$Pd_{40}\ Cu_{40}\ P_{20}$	[24]	[110]	US	⊙
$Pd_{39}\ Ni_{10}\ Cu_{30}\ P_{21}$	[24]	[7]*	US	⊙
$Fe_{53}\ Cr_{15}\ Mo_{14}\ Er_1\ C_{15}\ B_6$	[24]	[109]	US	⊙
$Fe_{61}\ Mn_{10}\ Cr_4\ Mo_6\ Er_1\ C_{15}\ B_6$	[24]	[109]	US	⊙
DC704	[19]	[19]	PUI	⊙
Glycerol	[19]	[19]	PUI	⊙
Corning Jade glass	[29]	[29]	BRI	⊗

Through a rather complicated protocol, both experimentally and theoretically, the conclusion was that the dependence of the shear modulus on temperature and fictive temperature was not strong enough to explain the change in viscosity for the examined oxide glass. This work confirmed previous findings by the same group [30].

4. Concluding remarks

In Table 1 we have compiled all the tests of the shoving model we have identified by searching the scientific literature. The table is ordered chronologically. Each system tested in a given publication is listed along with the reference to the paper from which the data used for the test was taken (of course, often the two are identical). To test the model two sets of data are needed, e.g., viscosity and G_∞ or fragility index and mean-square displacement, etc. Thus there may be several references for the same substance. The last column states by which method the mechanical data were obtained.

Many systems studied confirm the model prediction. We find no correlation to the chemistry of the liquids; agreement with the shoving model has been reported for van der Waals bonded liquids, metal glasses, oxide glasses, as well as for hydrogen-bonded liquids. The liquids reported not to obey the model prediction also do not show any particular pattern with respect to chemistry or otherwise. The only clear trend is that within a given publication the conclusion is often the same for more or less all liquids studied, whether in agreement with the model (e.g., Refs. [1,18]), or contradicting the model (e.g., Refs. [23,29]).

Several liquids occur more than once in the table (for instance the silicone oil DC704 in Refs. [1,26,18,19] and glycerol in Refs. [25,22,31,19]). This is because of different measurement methods or different kinds of tests being used. A few liquids are found to be in agreement with the model in one test, but not when using a different technique. This stresses the fact that measuring the mechanical properties of a liquid is difficult to do reliably.

Testing the model's ability to capture the non-Arrhenius temperature dependence of the relaxation time rather than just looking at a single temperature gives a more quantitative impression of its validity. In particular, tests that involve fragility indices and other measures involving derivatives and extrapolations may give a misguided picture, because of the significant uncertainties often associated with these quantities. Ideally, all quantities entering the test should be measured simultaneously or at least under identical experimental conditions. These demands give the rheological tests more weight, since these are the only methods that are able to determine both the long-time properties (relaxation time or viscosity) and the short-time properties (G_∞) in the same measurement (albeit, sometimes under the assumption of TTS). On the other hand, if one wants to make sure that it is really the high-frequency plateau of the mechanical properties that is being measured, sound velocity measurements at frequencies up to tens of GHz offer a better alternative.

This paper focused on experimental tests of the shoving model, not on theoretical developments, but one very recent such development deserves to be mentioned. This is the first-principles theory developed by Mirigian and Schweizer [32–34] that combines their previous force-level nonlinear Langevin equation theory of single-particle hopping with the contribution to the energy barrier deriving from the shoving work. The new model has no adjustable parameters but is nevertheless able to explain relaxation time data over 14 decades for nonpolar molecules, alcohols, rare gases and liquid metals (less so for hydrogen-bonded systems, though). In the Mirigian–Schweizer theory the shoving work dominates the energy barrier at low temperatures, i.e., for relatively large relaxation times.

Our overall conclusion is the following: The shoving model offers a straightforward explanation of the cause of the mysterious super-Arrhenius temperature dependence of glass-forming liquids' relaxation time. There are not yet enough reliable data to determine the model's range of applicability. In conjunction, these two things point to the need for more work on obtaining reliable data for the high-frequency mechanical properties of supercooled liquids.

Acknowledgments

The center for viscous liquid dynamics "Glass and Time" is sponsored by the Danish National Research Foundation via grant DNRF61.

References

[1] J.C. Dyre, N.B. Olsen, T. Christensen, Local elastic expansion model for viscous-flow activation energies of glass-forming molecular liquids, Phys. Rev. B 53 (1996) 2171–2174.
[2] J.C. Dyre, The glass transition and elastic models of glass-forming liquids, Rev. Mod. Phys. 78 (3) (2006) 953–972.
[3] M. Goldstein, Viscous liquids and the glass transition: a potential energy barrier picture, J. Chem. Phys. 51 (1969) 3728–3739.
[4] T.B. Schrøder, S. Sastry, J. Dyre, S.C. Glotzer, Crossover to potential energy landscape dominated dynamics in a model glass-forming liquid, J. Chem. Phys. 112 (22) (2000) 9834–9840.
[5] N. Gnan, T.B. Schrøder, U.R. Pedersen, N.P. Bailey, J.C. Dyre, Pressure–energy correlations in liquids. IV. 'Isomorphs' in liquid state diagrams, J. Chem. Phys. 131 (2009) 234504.
[6] F. Puosi, D. Leporini, Communication: correlation of the instantaneous and the intermediate-time elasticity with the structural relaxation in glassforming systems, J. Chem. Phys. 136 (4) (2012) 041104 (URL http://scitation.aip.org/content/aip/journal/jcp/136/4/10.1063/1.3681291).
[7] W.H. Wang, The elastic properties, elastic models and elastic perspectives of metallic glasses, Prog. Mater. Sci. 57 (2012) 487.
[8] B. Jakobsen, K. Niss, N.B. Olsen, Dielectric and shear mechanical alpha and beta relaxations in seven glass-forming liquids, J. Chem. Phys. 123 (23) (2005) 234511.
[9] C. Maggi, B. Jakobsen, T. Christensen, N.B. Olsen, J.C. Dyre, Supercooled liquid dynamics studied via shear-mechanical spectroscopy, J. Phys. Chem. B 112 (2008) 16320–16325.
[10] T. Christensen, N.B. Olsen, A rheometer for the measurement of high shear modulus covering more than seven decades of frequency below 50 kHz, Rev. Sci. Instrum. 66 (10) (1995) 5019–5031.
[11] J.C. Dyre, T.E. Christensen, N.B. Olsen, Elastic models for the non-Arrhenius viscosity of glass-forming liquids, J. Non-Cryst. Solids 352 (2006) 4632–4642.
[12] C. Gainaru, T. Hecksher, N.B. Olsen, R. Böhmer, J.C. Dyre, Shear and dielectric responses of propylene carbonate, tripropylene glycol and a mixture of two secondary amides, J. Chem. Phys. 137 (2012) 064508.
[13] B. Xu, G.B. McKenna, Evaluation of the Dyre shoving model using dynamic data near the glass temperature, J. Chem. Phys. 134 (2011) 124902.
[14] L.D. Landau, E.M. Lifshitz, Theory of Elasticity, Elsevier, 1986.
[15] L. Comez, D. Fioretto, F. Scarponi, G. Monaco, Density fluctuations in the intermediate glass-former glycerol: a Brillouin light scattering study, J. Chem. Phys. 119 (12) (2003) 6032–6043 (URL http://scitation.aip.org/content/aip/journal/jcp/119/12/10.1063/1.1601608).
[16] K. Venkateshan, J.P. Johari, Dielectric relaxation and elasticity during polymerization, J. Chem. Phys. 125 (2006) 014907.
[17] G. Harrison, The Dynamic Properties of Supercooled Liquids, Academic Press, 1976.
[18] D.H. Torchinsky, J.A. Johnson, K.A. Nelson, A direct test of the correlation between elastic parameters and fragility of ten glass formers and their relationship to elastic models of the glass transition, J. Chem. Phys. 130 (2009) 064502.
[19] C. Klieber, T. Hecksher, T. Pezeril, D.H. Torchinsky, J.C. Dyre, K.A. Nelson, Mechanical spectra of viscous liquids. II. Gigahertz-frequency longitudinal and shear acoustic dynamics in glycerol and dc704 studied by time-domain Brillouin scattering, J. Chem. Phys. 138 (2013) 12A544.
[20] J.C. Dyre, N.B. Olsen, Landscape equivalent of the shoving model, Phys. Rev. E. 69 (2004) 042501.
[21] T. Hecksher, A.I. Nielsen, N.B. Olsen, J.C. Dyre, Little evidence for dynamic divergences in ultraviscous molecular liquids, Nat. Phys. 4 (9) (2008) 737–741.
[22] K. Niss, C. Dalle-Ferrier, B. Frick, D. Russo, J.C. Dyre, C. Alba-Simionesco, Connection between slow and fast dynamics of molecular liquids around the glass transition, Phys. Rev. B 82 (2010) 021508.
[23] L. Larini, A. Ottochian, C. de Michele, D. Leporini, Universal scaling between structural relaxation and vibrational dynamics in glass-forming liquids and polymers, Nat. Phys. 4 (2008) 42.
[24] J.C. Dyre, W.-H. Wang, The instantaneous shear modulus in the shoving model, J. Chem. Phys. 136 (2012) 224108.
[25] U. Buchenau, Fragility and elasticity: description of flow in highly viscous liquids, Phys. Rev. B 80 (2009) 172201.
[26] N.B. Olsen, J.C. Dyre, T.E. Christensen, Structural relaxation monitored by instantaneous shear modulus, Phys. Rev. Lett. 81 (1998) 1031–1033.
[27] A.Q. Tool, C.G. Eichlin, Variations caused in the heating curves of glass by heat treatment, J. Am. Cer. Soc 14 (4) (1931) 276–308.
[28] O.S. Narayanaswamy, A model of structural relaxation in glass, J. Am. Ceram. Soc. 54 (10) (1971) 491–498.
[29] M. Potuzak, X. Guo, M.M. Smedskjaer, J.C. Mauro, Are the dynamics of a glass embedded in its elastic properties? J. Chem. Phys. 138 (2013) 12A501.

[30] M.M. Smedskjaer, L. Huang, G. Scannell, J.C. Mauro, Elastic interpretation of the glass transition in aluminosilicate liquids, Phys. Rev. B 85 (14) (2012) 144203 (URL http://prb.aps.org/abstract/PRB/v85/i14/e144203).
[31] T. Rouxel, Thermodynamics of viscous flow and elasticity of glass forming liquids in the glass transition range, J. Chem. Phys. 135 (2011) 184501, http://dx.doi.org/10.1063/1.3656695.
[32] S. Mirigian, K.S. Schweizer, Unified theory of activated relaxation in liquids over 14 decades in time, J. Phys. Chem. Lett. 4 (21) (2013) 3648–3653 (URL http://pubs.acs.org/doi/abs/10.1021/jz4018943).
[33] S. Mirigian, K.S. Schweizer, Elastically cooperative activated barrier hopping theory of relaxation in viscous fluids. i. General formulation and application to hard sphere fluids, J. Chem. Phys. 140 (19) (2014) 194506 (URL http://scitation.aip.org/content/aip/journal/jcp/140/19/10.1063/1.4874842).
[34] S. Mirigian, K.S. Schweizer, Elastically cooperative activated barrier hopping theory of relaxation in viscous fluids. ii. Thermal liquids, J. Chem. Phys. 140 (19) (2014) 194507 (URL http://scitation.aip.org/content/aip/journal/jcp/140/19/10.1063/1.4874843).
[35] A.J. Barlow, J. Lamb, A.J. Matheson, P.R.K. Padmini, J. Richter, Viscoelastic relaxation of supercooled liquids. I, Proc. R. Soc. Lond. A 298 (1455) (1967) 467–480.
[36] C.T. Moynihan, P.B. Macedo, C.J. Montrose, P.K. Gupta, M.A. DeBolt, J.F. Jill, B.E. Dom, P.W. Drake, A.J. Easteal, P.B. Elterman, R.P. Moeller, H. Sasabe, J.A. Wilder, Structural relaxation in vitreous materials, Ann. N. Y. Acad. Sci. 279 (1976) 15–35.
[37] C.H. Wang, R.-J. Ma, Q.-L. Liu, Depolarized light scattering from shear wave in a viscoelastic liquid: alpha-phenyl o-cresol, J. Chem. Phys. 80 (2) (1984) 617–625.
[38] W.T. Laughlin, D.R. Uhlmann, Viscous flow in simple organic liquids, J. Phys. Chem. 76 (16) (1972) 2317–2325.
[39] A. Bains, C. Gordon, A. Granato, R. Schwarz, The shear modulus of bulk amorphous $Pd_{40}Ni_{40}P_{20}$ and its relation to viscosity and specific heat, J. Alloys Compd. 310 (1) (2000) 20–23.
[40] M.L. Lind, G. Duan, W.L. Johnson, Isoconfigurational elastic constants and liquid fragility of a bulk metallic glass forming alloy, Phys. Rev. Lett. 97 (2006) 015501.
[41] R.H. Doremus, Viscosity of silica, J. Appl. Phys. 92 (2002) 7619–7629.
[42] A. Wischnewski, Kohärent inelastische neutronenstreuung an gläsern, (Ph.D. thesis) Heinrich-Heine Universität, 1998.
[43] K.M. Bernatz, I. Echeverria, S.L. Simon, D.J. Plazek, Viscoelastic properties of boron dioxide, J. Non-Cryst. Solids 289 (2001) 9–16.
[44] D. Sidebottom, R. Bergman, L. Börjesson, L.M. Torell, Two-step relaxation decay in a strong glass-former, Phys. Rev. Lett. 71 (1993) 2260–2263.
[45] D. Engberg, A. Wischnewski, U. Buchenau, L. Börjesson, A.J. Dianoux, A.P. Sokolov, L. M. Torell, Sound waves and other modes in the strong glass-former B_2O_3, Phys. Rev. B 58 (1998) 9087–9097.
[46] R. Busch, E. Bakke, W.L. Johnson, Viscosity of the supercooled liquid and relaxation at the glass transition of the $Zr_{46.8}Ti_{8.2}Cu_{7.5}Ni_{10}Be_{27.5}$ bulk metallic glass-forming alloy, Acta Mater. 46 (1998) 4725–4732.
[47] A. Meyer, H. Franz, S. B., W. J., W. Petry, Fast relaxation in a metastable melt, Europhys. Lett. 36 (1996) 379–384.
[48] H.Z. Cummins, J. Hernandez, W.M. Du, G. Li, Anomalies in the scaling of the dielectric α-relaxation, Phys. Rev. Lett. 73 (1994) 2935-2935.
[49] J. Wuttke, W. Petry, G. Coddens, F. Fujara, Fast dynamics of glass-forming glycerol, Phys. Rev. E. 52 (1995) 4026–4034.
[50] C.M. Roland, M.J. Schroeder, J.J. Fontanella, K.L. Ngai, Evolution of the dynamics in 1,4-polyisoprene from a nearly constant loss to a Johari–Goldstein β-relaxation to the α-relaxation, Macromolecules 37 (2004) 2630–2635.
[51] B. Frick, L.J. Fetters, Methyl group dynamics in glassy polysisoprene: a neutron back-scattering investigation, Macromolecules 27 (1994) 974–980.
[52] D.J. Plazek, J.H. Magill, Physical properties of aromatic hydrocarbons. IV. An analysis of the temperature dependence of the viscosity and the compliance of 1,3,5 tri-α-naphthylbenzene, J. Chem. Phys. 49 (8) (1968) 3678–3682 (URL http://scitation.aip.org/content/aip/journal/jcp/49/8/10.1063/1.1670651).
[53] K.L. Ngai, Dynamic and thermodynamic properties of glass-forming substances, J. Non-Cryst. Solids 275 (1–2) (2000) 7–51.
[54] N. Menon, S.R. Nagel, D.C. Venerus, Dynamics viscosity of a simple glass-forming liquid, Phys. Rev. Lett. 73 (1994) 963–966.
[55] H. Franz, W. Petry, A.Q.R. Baron, Quasielastic scattering: slow dynamics of glasses, Hyperfine Interact. 123 (1–4) (1999) 865–879 (URL http://link.springer.com/article/10.1023/A:1017013015981).
[56] A. Tölle, Neutron scattering studies of the model glass former ortho-terphenyl, Rep. Prog. Phys. 64 (11) (2001) 1473 (URL http://iopscience.iop.org/0034-4885/64/11/203).
[57] U. Buchenau, R. Zorn, A relation between fast and slow motions in glassy and liquid selenium, EPL Europhys. Lett. 18 (6) (1992) 523 (URL http://iopscience.iop.org/0295-5075/18/6/009).
[58] R. Zorn, Microscopic dynamics of glass-forming polymers, J. Phys. Condens. Matter 15 (23) (2003) R1025 (URL http://iopscience.iop.org/0953-8984/15/23/201).
[59] B. Frick, D. Richter, The microscopic basis of the glass transition in polymers from neutron scattering studies, Science 267 (5206) (1995) 1939–1945 (URL http://www.sciencemag.org/content/267/5206/1939.short).
[60] B. Frick, D. Richter, W. Petry, U. Buchenau, Study of the glass transition order parameter in amorphous polybutadiene by incoherent neutron scattering, Z. Phys. B Condensed Matter 70 (1) (1988) 73–79 (URL http://link.springer.com/article/10.1007/BF01320541).
[61] C.M. Roland, K.L. Ngai, P.G. Santangelo, X.H. Qiu, M.D. Ediger, D.J. Plazek, Temperature dependence of segmental and terminal relaxation in atactic polypropylene melts, Macromolecules 34 (18) (2001) 6159–6160 (URL http://pubs.acs.org/doi/pdf/10.1021/ma002121p).
[62] T. Kanaya, K. Kaji, J. Bartos, M. Klimova, Onset of the fast process in amorphous polypropylene as detected by quasielastic neutron-scattering and electron spin resonance techniques, Macromolecules 30 (4) (1997) 1107–1110 (URL http://pubs.acs.org/doi/abs/10.1021/ma960563o).
[63] R.H. Colby, Dynamic scaling approach to glass formation, Phys. Rev. E. 61 (2) (2000) 1783 (URL http://pre.aps.org/abstract/PRE/v61/i2/p1783_1).
[64] C.L. Soles, J.F. Douglas, W.-L. Wu, R.M. Dimeo, Incoherent neutron scattering as a probe of the dynamics in molecularly thin polymer films, Macromolecules 36 (2) (2003) 373–379 (URL http://pubs.acs.org/doi/abs/10.1021/ma020952k).
[65] N. McCrum, B. Read, G. Williams, Anelastic and Dielectric Effects in Solid Polymers, Dover, New York, 1991.
[66] P.K. Dixon, L. Wu, S.R. Nagel, B.D. Williams, J.P. Carini, Scaling in the relaxation of supercooled liquids, Phys. Rev. Lett. 65 (1990) 1108–1111.
[67] M. Cutroni, A. Mandanici, A. Piccolo, The dielectric-relaxation behavior of *m*-fluoroaniline above the glass-transition, J. Phys. Condens. Matter 7 (34) (1995) 6781–6788.
[68] H.P. Zhang, A. Brodin, H.C. Barshilia, G.Q. Shen, H.Z. Cummins, R.M. Pick, Brillouin scattering study of salol: exploring the effects of rotation-translation coupling, Phys. Rev. E. 70 (1) (2004) 011502.
[69] M. Cutroni, A. Mandanici, The α-relaxation process in simple glass forming liquid *m*-toluidine. II. The temperature dependence of the mechanical response, J. Chem. Phys. 114 (2001) 7124–7129.
[70] A. Mandanici, R. Richert, M. Cutroni, X. Shi, S.A. Hutcheson, G.B. McKenna, Relaxational features of supercooled and glassy *m*-toluidine, J. Non-Cryst. Solids 352 (2006) 4729–4734.
[71] A. Drozd-Rzoska, S.J. Rzoska, Derivative-based analysis for temperature and pressure evolution of dielectric relaxation times in vitrifying liquids, Phys. Rev. E Stat. Nonlinear Soft Matter Phys. 73 (4) (2006) 041502.
[72] M. Mizukami, K. Kobashi, M. Hanaya, M. Oguni, Presence of two freezing-in processes concerning alpha-glass transition in the new liquid phase of triphenyl phosphite and its consistency with "cluster structure" and "intracluster rearrangement for alpha process" models, J. Phys. Chem. B 103 (20) (1999) 4078–4088.
[73] D.R. Macfarlane, D.K.Y. Wong, Conductivity and dielectric-relaxation in calcium nitrate tetrahydrate and sodium thiosulfate pentahydrate near T_g, J. Chem. Phys. 89 (26) (1985) 5849–5855.
[74] V.A. Khonik, Y.P. Mitrofanov, S.A. Lyakhov, A.N. Vasiliev, S.V. Khonik, D.A. Khoviv, Relationship between the shear modulus *G*, activation energy, and shear viscosity η in metallic glasses below and above T_g: Direct in situ measurements of *G* and η, Phys. Rev. B 79 (2009) 132204.
[75] J. Mills, Low frequency storage and loss moduli of soda-silica glasses in the transformation range, J. Non-Cryst. Solids 14 (1974) 255–268, http://dx.doi.org/10.1016/0022-3093(74)90034-9.
[76] J.A. Bucaro, H.D. Dardy, High-temperature Brillouin scattering in fused quartz, J. Appl. Phys. 45 (12) (1974) 5324–5329 (URL http://scitation.aip.org/content/aip/journal/jap/45/12/10.1063/1.1663238).
[77] F. Scarponi, L. Comez, D. Fioretto, L. Palmieri, Brillouin light scattering from transverse and longitudinal acoustic waves in glycerol, Phys. Rev. B 70 (2004) 054203.
[78] R. Böhmer, K.L. Ngai, C.A. Angell, D.J. Plazek, Nonexponential relaxation in strong and fragile glass-formers, J. Chem. Phys. 99 (1993) 4201.
[79] K. Schröter, E. Donth, Viscosity and shear response at the dynamic glass transition of glycerol, J. Chem. Phys. 113 (2000) 9101–9108 (URL http://adsabs.harvard.edu/abs/2000JChPh.113.9101S).
[80] V.N. Novikov, A.P. Sokolov, B. Strube, N.V. Surovtsev, E. Duval, A. Mermet, Connection between quasielastic Raman scattering and free volume in polymeric glasses and supercooled liquids, J. Chem. Phys. 107 (4) (1997) 1057–1065 (URL http://scitation.aip.org/content/aip/journal/jcp/107/4/10.1063/1.474453).
[81] D.W. van Krevelen, Properties of Polymers, Elsevier, New York, 1976.
[82] K. Niss, B. Jakobsen, N.B. Olsen, Dielectric and shear mechanical relaxations in glass-forming liquids: a test of the Gemant–DiMarzio–Bishop model, J. Chem. Phys. 123 (2005) 234510.
[83] L.M. Torell, R. Aronsson, Brillouin scattering study of elastic properties in a glass forming KNO_3–Ca $(NO_3)_2$ mixture, J. Chem. Phys. 78 (3) (1983) 1121–1125 (URL http://scitation.aip.org/content/aip/journal/jcp/78/3/10.1063/1.444896).
[84] G.D. Patterson, Brillouin scattering from amorphous bisphenol-a polycarbonate, J. Polym. Sci. Polym. Phys. Ed. 14 (4) (1976) 741–747 (URL http://onlinelibrary.wiley.com/doi/10.1002/pol.1976.180140413/full).
[85] K. Mpoukouvalas, N. Gomopoulos, G. Floudas, C. Herrmann, A. Hanewald, A. Best, Effect of pressure on the segmental dynamics of bisphenol-a-polycarbonate, Polymer 47 (20) (2006) 7170–7177.
[86] Y. Takagi, T. Hosokawa, K. Hoshikawa, H. Kobayashi, Y. Hiki, Relaxation of polystyrene near the glass transition temperature studied by acoustic measurements, J. Phys. Soc. Jpn. 76 (2) (2007) http://journals.jps.jp/doi/abs/10.1143/JPSJ.76.024604.
[87] A. Sahnoune, F. Massines, L. Piche, Ultrasonic measurement of relaxation behavior in polystyrene, J. Polym. Sci. B Polym. Phys. 34 (2) (1996) 341–348 (URL http://onlinelibrary.wiley.com/doi/10.1002/(SICI)1099-0488(19960130)34:2%3C341::AID-POLB15%3E3.0.CO;2-J/abstract).
[88] E. Donth, M. Beiner, S. Reissig, J. Korus, F. Garwe, S. Vieweg, S. Kahle, E. Hempel, K. Schröter, Fine structure of the main transition in amorphous polymers: entanglement spacing and characteristic length of the glass transition. Discussion of examples, Macromolecules 29 (20) (1996) 6589–6600 (URL http://pubs.acs.org/doi/abs/10.1021/ma951881a).
[89] J.K. Kruger, R. Roberts, H.G. Unruh, K.P. Fruhauf, J. Helwig, H.E. Muser, A reinvestigation of the hypersonic properties and the specific-heat of PMMA around the quasi-static glass-transition. 1. High-performance Brillouin investigations, Progr. Colloid Polym. Sci. 71 (1985) 77–85.
[90] J. Perez, J.Y. Cavaille, L. David, New experimental features and revisiting the α and β mechanical relaxation in glasses and glass-forming liquids, J. Mol. Struct. 479 (2) (1999) 183–194.

[91] R. Richert, K. Duvvuri, L.-T. Duong, Dynamics of glass-forming liquids. VII. Dielectric relaxation of supercooled tris-naphthylbenzene, squalane and decahydroisoquinoline, J. Chem. Phys. 118 (4) (2003) 1828–1836.
[92] R. Casalini, M.J. McGrath, C.M. Roland, Isobaric and isochoric properties of decahydroisoquinoline, an extremely fragile glass-former, J. Non-Cryst. Solids 352 (2006) 4905–4909.
[93] A.J. Barlow, J. Lamb, A.J. Matheson, Viscous behaviour of supercooled liquids, Proc. R. Soc. London Ser. A 292 (1430) (1966) 322–342.
[94] N.B. Olsen, T. Christensen, J.C. Dyre, Time–temperature superposition in viscous liquids, Phys. Rev. Lett. 86 (7) (2001) 1271–1274.
[95] N.B. Olsen, Scaling of β-relaxation in the equilibrium liquid state of sorbitol, J. Non-Cryst. Solids 235–237 (1998) 399–405.
[96] S.A. Hutcheson, G.B. McKenna, The measurement of mechanical properties of glycerol, *m*-toluidine, and sucrose benzoate under consideration of corrected theometer compliance: an in-depth study and review, J. Chem. Phys. 129 (2008) 074502.
[97] Y. Gueguen, T. Rouxel, P. Gadaud, C. Bernard, V. Keryvin, J.-C. Sangleboeuf, High-temperature elasticity and viscosity of GexSe1-x glasses in the transition range, Phys. Rev. B: Condens. Matter Mater. Phys. 84 (6) (2011) 064201 (URL http://journals.aps.org/prb/abstract/10.1103/PhysRevB.84.064201).
[98] P. Gadaud, S. Pautrot, Characterization of the elasticity and anelasticity of bulk glasses by dynamical subresonant and resonant techniques, J. Non-Cryst. Solids 316 (1) (2003) 146–152 (URL http://www.sciencedirect.com/science/article/pii/S0022309302019476).
[99] W.M. Slie, A.R. Donfor Jr., T.A. Litovitz, Ultrasonic shear and longitudinal measurements in aqueous glycerol, J. Chem. Phys. 44 (10) (1966) 3712–3718 (RL http://scitation.aip.org/content/aip/journal/jcp/44/10/10.1063/1.1726524).
[100] T. Rouxel, Elastic properties and short-to medium-range order in glasses, J. Am. Ceram. Soc. 90 (10) (2007) 3019–3039 (URL http://onlinelibrary.wiley.com/doi/10.1111/j.1551-2916.2007.01945.x/full).
[101] C.C. Chen, Y.J. Wu, L.G. Hwa, Temperature dependence of elastic properties of zblan glasses, Mater. Chem. Phys. 65 (3) (2000) 306–309.
[102] R.E. Youngman, J. Kieffer, J.D. Bass, L. Duffrene, Extended structural integrity in network glasses and liquids, J. Non-Cryst. Solids 222 (1997) 190–198 (URL http://www.sciencedirect.com/science/article/pii/S0022309397901137).
[103] V. Askarpour, M.H. Manghnani, P. Richet, Elastic properties of diopside, anorthite, and grossular glasses and liquids: a Brillouin scattering study up to 1400 k, J. Geophys. Res. 98 (B10) (1993) 17683–17689 (URL http://onlinelibrary.wiley.com/doi/10.1029/93JB01558/full).
[104] V. Keryvin, T. Rouxel, M. Huger, L. Charleux, Elastic moduli of a ZrCuAlNi bulk metallic glass from room temperature to complete crystallisation by in situ pulse-echo ultrasonic echography, J. Ceram. Soc. Jpn. 116 (1356) (2008) 851–854 (URL http://jlc.jst.go.jp/JST.JSTAGE/jcersj2/116.851?from=Google).
[105] K. Tanaka, T. Ichitsubo, E. Matsubara, Elasticity and anelasticity of metallic glass near the glass transition temperature, Mater. Sci. Eng. A 442 (1) (2006) 278–282 (URL http://www.sciencedirect.com/science/article/pii/S0921509306010471).
[106] T. Rouxel, J.-C. Sangleboeuf, The brittle to ductile transition in a soda–lime–silica glass, J. Non-Cryst. Solids 271 (3) (2000) 224–235 (URL http://www.sciencedirect.com/science/article/pii/S0022309300001095).
[107] H. Lemercier, T. Rouxel, D. Fargeot, J.-L. Besson, B. Piriou, Yttrium sialon glasses: structure and mechanical properties — elasticity and viscosity, J. Non-Cryst. Solids 201 (1) (1996) 128–145 (URL http://www.sciencedirect.com/science/article/pii/0022309396001470).
[108] L. Donzel, A. Lakki, R. Schaller, Glass transition and α relaxation in y–si–al–o–n glasses and in si3n4 ceramics studied by mechanical spectroscopy, Philos. Mag. A 76 (5) (1997) 933–944 (URL http://www.tandfonline.com/doi/abs/10.1080/01418619708200008).
[109] J.Q. Wang, W.H. Wang, Y.H. Liu, H.Y. Bai, Characterization of activation energy for flow in metallic glasses, Phys. Rev. B 83 (2011) 012201.
[110] W.H. Wang, Elastic moduli and behaviors of metallic glasses, J. Non-Cryst. Solids 351 (16) (2005) 1481–1485.
[111] W.H. Wang, Correlations between elastic moduli and properties in bulk metallic glasses, J. Appl. Phys. 99 (9) (2006) 093506 (URL http://scitation.aip.org/content/aip/journal/jap/99/9/10.1063/1.2193060).